Determination of the neutrino mass hierarchy via the phase of the disappearance oscillation probability with a monochromatic $\bar{\nu}_e$ source

H. Minakata,[1,*] H. Nunokawa,[2,†] S. J. Parke,[3,‡] and R. Zukanovich Funchal[4,§]

[1]*Department of Physics, Tokyo Metropolitan University, Hachioji, Tokyo 192-0397, Japan*
[2]*Departamento de Física, Pontifícia Universidade Católica do Rio de Janeiro, C.P. 38071, 22452-970, Rio de Janeiro, Brazil*
[3]*Theoretical Physics Department, Fermi National Accelerator Laboratory, P.O. Box 500, Batavia, Illinois 60510, USA*
[4]*Instituto de Física, Universidade de São Paulo, C.P. 66.318, 05315-970 São Paulo, Brazil*

The neutrino mass hierarchy can be determined, in principle, by measuring a phase in the disappearance oscillation probability in vacuum, without relying on the matter effect, using a single channel. This phase is not the same for the normal and inverted neutrino mass spectra. In this paper, we give a complete description and physics understanding of the method. The key feature of the method is to detect advancement (normal) or retardation (inverted) of the phase of the atmospheric-scale oscillation relative to the solar-scale oscillation. We then show that this method can be realized with the recently proposed resonant $\bar{\nu}_e$ absorption reaction enhanced by the Mössbauer effect. The unique feature of this setup is the ultramonochromaticity of the observed $\bar{\nu}_e$'s. Because of this feature, the phase advancement or retardation of atmospheric-scale neutrino oscillation is detectable after 20 or more oscillations if the source and the target are made sufficiently compact in size. A quantitative estimate of the sensitivity to mass hierarchy resolution is given. We have also examined how a possible continuation of such an experiment can be carried out in order also to achieve high precision (few percent) determination of the solar-scale oscillation parameters Δm_{21}^2 and θ_{12}.

I. INTRODUCTION

Among the remaining unknowns in neutrino physics, resolving the neutrino mass hierarchy may be one of key importance to our understanding of physics of neutrino masses and the lepton flavor mixing [1]. Given the significance of the problem, it is natural that many methods are proposed for determining the mass hierarchy. The most conventional one would be to do neutrino and antineutrino comparison in long-baseline accelerator based oscillation experiments [2,3]. Because of the difference in how the matter effect interferes with the vacuum oscillation effect, it can signal the sign of Δm_{31}^2, and hence the mass hierarchy. Other less conventional ideas include the methods using atmospheric neutrinos [4], ν_e and ν_μ disappearance channels [5–7], supernova neutrinos [8,9], and neutrinoless double beta decay [10]. These lists of references cannot be complete, and some of the other relevant references are quoted therein.

In this paper, we discuss yet another way of determining the neutrino mass hierarchy by a neutrino oscillation disappearance experiment using *a single neutrino flavor* in vacuum, whereas in previous works [6,7] the method required the use of two different disappearance channels close to the first oscillation maximum. The pos-

sibility that the neutrino survival probability in vacuum can be sensitive to the neutrino mass hierarchy was first suggested in [11] using reactor neutrinos in the context of high-Δm^2 large mixing angle solar neutrino solution. It was also pursued recently in the Hanohano project using a Fourier transform technique [12]. We present here a complete formulation and physics understanding of the new method to determine the neutrino mass hierarchy.

This method utilizes the feature that the atmospheric-Δm^2 scale oscillation ''interferes'' with the solar-Δm^2 scale oscillation in a different way depending upon the mass hierarchy. We first carefully reformulate the difference as an advancement or retardation of the phase of the atmospheric-scale neutrino oscillation relative to the solar-scale oscillation; for the ν_e and $\bar{\nu}_e$ disappearance probabilities, the atmospheric oscillation is continuously advanced (retarded) for the normal (inverted) hierarchy. Since the core of the problem exists in extracting long wavelength solar oscillation out of the two short wavelength atmospheric-scale oscillations due to Δm_{32}^2 and Δm_{31}^2, it is the critical matter to identify which quantity to be held fixed in defining the mass hierarchy reversal from the normal to the inverted, or vice versa. To our understanding, the only known appropriate quantity to hold is the effective neutrino mass squared difference Δm_{ee}^2 [see Eq. (4)], the one which is actually observed in ν_e (or $\bar{\nu}_e$) disappearance measurement at the first few oscillation maxima and/or minima [6]. We find it important to have the proper formalism because otherwise the sensi-

*minakata@phys.metro-u.ac.jp
†nunokawa@fis.puc-rio.br
‡parke@fnal.gov
§zukanov@if.usp.br

tivity to the mass hierarchy resolution can be significantly overestimated.

Then, we point out that an experiment using the resonant $\bar{\nu}_e$ absorption reaction [13] enhanced by the Mössbauer effect recently proposed by Raghavan [14] gives the first concrete realization of the idea. (See [15] for earlier proposals of Mössbauer enhanced experiments.) Because of the monochromaticity of the $\bar{\nu}_e$ beam from the bound-state beta decay [16], the phase advancement or retardation of atmospheric-scale neutrino oscillation is detectable after 20 or more oscillations if the source and the target are made sufficiently compact in size. The unique feature of this method is the use of this ultramonochromatic neutrino source thereby sidestepping the very high energy resolution requirement requested with reactor or accelerator neutrinos.

A concrete plan for the experiment may be as follows; in the first stage the atmospheric Δm_{ee}^2 must be accurately measured in a way described in [17] by a measurement at ~ 10 m baseline. As we will see, the precision of the measurement must reach subpercent level in order for this method to work. Then, in the second-stage relative phase advancement or retardation of the atmospheric-scale neutrino oscillation must be detected by moving the detector to ~ 350 m, this is just beyond the solar-scale oscillation distance for 18.6 keV neutrinos. Based on this plan, we give a detailed estimate of the sensitivity to the resolution of the mass hierarchy.

Upon finishing the above measurement, it is natural to think about the continuation of the experiment by moving the detector to distances tuned for precision measurement of the oscillation parameters relevant for solar neutrinos, Δm_{21}^2 and θ_{12}. We also give a detailed estimate of the accuracy for the determination of these parameters. It is notable that a resonant $\bar{\nu}_e$ absorption experiment could allow to make precise measurements of *all mixing parameters* that appear in the $\nu_e \rightarrow \nu_e$ oscillation channel: θ_{13}, θ_{12}, Δm_{21}^2, the effective atmospheric Δm_{ee}^2, and the neutrino mass hierarchy.

In Sec. II, we first describe the essence of the method in an explanatory way. We then define our theoretical machinery using the effective Δm_{ee}^2. We also clarify the basic requirement for the measurement. In Sec. III, we discuss the concrete setup of the experiment and describe our statistical method for the analysis. We then give the analysis results on sensitivity to the mass hierarchy resolution. In Sec. IV, we describe the analysis for the determination of the solar oscillation parameters. In Sec. V, we finish by giving our concluding remarks. In Appendix A, we give a different interpretation of the phenomena in terms of the effective mass squared differences, whereas in Appendix B we discuss how this method can be applied to the ν_μ disappearance channel. This possibility has been discussed in [18]; however, the baseline required is $L \simeq 11\,000(E/0.6\,\text{GeV})\,\text{km}$.

II. HOW CAN ν_e DISAPPEARANCE MEASUREMENT ALONE SIGNAL THE NEUTRINO MASS HIERARCHY?

The vacuum ν_e survival probability using $\Delta_{ij} \equiv \Delta m_{ij}^2 L/4E$ ($\Delta m_{ij}^2 \equiv m_i^2 - m_j^2$) as shorthand for the kinematical phase, can be written without any approximation as

$$
\begin{aligned}
P(\nu_e \rightarrow \nu_e) &= 1 - 4|U_{e3}|^2|U_{e1}|^2 \sin^2 \Delta_{31} \\
&\quad - 4|U_{e3}|^2|U_{e2}|^2 \sin^2 \Delta_{32} - P_\odot \\
&= 1 - \tfrac{1}{2}\sin^2 2\theta_{13}[1 - (c_{12}^2 \cos 2\Delta_{31} \\
&\quad + s_{12}^2 \cos 2\Delta_{32})] - P_\odot,
\end{aligned} \tag{1}
$$

where the usual parametrization of the mixing matrix [19] is used with the abbreviations $c_{ij} \equiv \cos\theta_{ij}$ and $s_{ij} \equiv \sin\theta_{ij}$. Here E is the neutrino energy and L is the baseline distance. $P_\odot$, as defined by

$$
P_\odot \equiv 4|U_{e2}|^2|U_{e1}|^2 \sin^2 \Delta_{21} = \sin^2 2\theta_{12} c_{13}^4 \sin^2 \Delta_{21}, \tag{2}
$$

is the oscillation probability associated with the solar Δm^2 scale. In this paper, we assume the standard three neutrino framework with *CPT* conservation (except for where we discuss possible *CPT* violation), which implies that Eq. (1) is also valid for $\bar{\nu}_e$.

The neutrino mass hierarchy can be determined if one knows which kinematical phase, $|\Delta_{31}|$ or $|\Delta_{32}|$, is larger. Namely, if $|\Delta_{31}| > |\Delta_{32}|$, the normal hierarchy is the case, and if $|\Delta_{31}| < |\Delta_{32}|$ the inverted one. How we can know which is larger? When two waves with slight different frequencies travel together there arises the phenomenon of beating. The amplitude of superposed waves beats with the frequency corresponding to the difference of two frequencies. For ν_e disappearance probability, Eq. (1), we have beating because the frequency of the two waves in (1) with $|\Delta_{31}|$ and $|\Delta_{32}|$ differ by the frequency associated with the $|\Delta_{21}|$ characterized by the solar Δm_{21}^2 scale, which is smaller by a factor of $\simeq 30$ compared to the atmospheric $|\Delta_{31}|$ scale. One can decompose the superposed waves into the beating low frequency wave and the high frequency wiggles within the beat. Here, unlike the case addressed in most textbooks of basic physics, the amplitude of the two frequencies is different. Therefore, to tell which of the high frequencies has a larger amplitude, one has to determine whether the phase of the high frequency wiggles advances or retards as the wave evolves. This phase advancement or retardation can tell us whether the neutrino mass hierarchy is normal or inverted using only the disappearance measurement in a single channel, $\nu_e \rightarrow \nu_e$ in vacuum.

To demonstrate that it is possible, we plot in the left panel of Fig. 1 the oscillation probability $P(\nu_e \rightarrow \nu_e)$ as a function of the distance L from a source. As one can clearly see in the figure, the case of normal hierarchy ($\Delta m_{31}^2 > 0$, blue curve, the advanced one) starts to be distinguished from the case of inverted hierarchy ($\Delta m_{31}^2 < 0$, red curve, the retarded one) at around $L \sim 300$ m because of the

advancement of the normal hierarchy's high frequency wiggles and the retardation of the inverted hierarchy's high frequency wiggles, i.e. the phase of the high frequency wiggles. What we mean by "beating" may be clearer in the left panel of Fig. 3 where the solar term is switched off.

To see the difference between the oscillation probabilities of the normal and the inverted hierarchies more clearly, we define the quantity

$$
\begin{aligned}
\Delta P(\nu_e \rightarrow \nu_e) &\equiv P(\nu_e \rightarrow \nu_e; \Delta m_{31}^2 > 0) \\
&- P(\nu_e \rightarrow \nu_e; \Delta m_{31}^2 < 0),
\end{aligned} \quad (3)
$$

where the hierarchy flip is defined so that $|\Delta P|$ is minimized for short baseline measurements. (See Sec. II A for the precise definition of the hierarchy flip.) We normalize ΔP by dividing by $\sqrt{P(\theta_{13} = 0)}$ since $P(\theta_{13} = 0)$ is the "background" for seeing θ_{13} effects in ν_e disappearance. The quantity $\Delta P/\sqrt{P(\theta_{13} = 0)}$ is plotted in the right panel of Fig. 1. The envelope of $|\Delta P|/\sqrt{P(\theta_{13} = 0)}$ slowly rises from 0 to a plateau value of $\sin^2 2\theta_{13}$ at a distance about 25% further from the source than the first solar oscillation maximum ($\Delta_{21} = \pi/2$ occurs when $L = 280$ m) and remains reasonably constant at this value beyond the first solar oscillation minimum ($\Delta_{21} = \pi$). Clearly, even though the difference between the hierarchies is very small at short distances, it becomes as large as theoretically possible, $\sin^2 2\theta_{13}$ (see below), at large distances.

A. Theoretical framework

To decompose the superposed waves into the beat and wiggle, one has to correctly define the high frequency mode. We choose to do this by defining a short distance effective Δm^2 in the ν_e disappearance channel, see [6]. It is given by

$$
\Delta m_{ee}^2 \equiv \cos^2 \theta_{12} |\Delta m_{31}^2| + \sin^2 \theta_{12} |\Delta m_{32}^2|. \quad (4)
$$

This is the only linear combination of Δm_{31}^2 and Δm_{32}^2 that can be determined by a short distance (over the first few atmospheric oscillations) ν_e disappearance experiment. Δm_{ee}^2 is defined to be positive for both hierarchies. The choice of the atmospheric Δm^2 is crucial; extraction of the low frequency mode can be done correctly only if the high frequency mode is identified in an appropriate way. See Sec. II C for more about it.

Now, we rewrite $P(\nu_e \rightarrow \nu_e)$ without any approximation, using the positive and measurable variables $\Delta_{ee} \equiv \Delta m_{ee}^2 L/4E$ and Δ_{21} and the phase $\phi_\odot$ (which will be given below), as follows:

$$
\begin{aligned}
P(\nu_e \rightarrow \nu_e) &= 1 - \tfrac{1}{2}\sin^2 2\theta_{13}[1 - \sqrt{1 - \sin^2 2\theta_{12}\sin^2\Delta_{21}} \\
&\times \cos(2\Delta_{ee} \pm \phi_\odot)] - P_\odot,
\end{aligned} \quad (5)
$$

where the positive (negative) *sign* in front of the phase $\phi_\odot$ corresponds to the normal (inverted) mass hierarchy; if Δm_{ee}^2 is precisely determined, the only effect of the hierarchy manifests itself as this *sign*. Clearly, the amplitude of the $\sin^2 2\theta_{13}$ oscillations is modulated by $\sqrt{1 - \sin^2 2\theta_{12}\sin^2\Delta_{21}}$ which varies from 1 to $\cos 2\theta_{12}$ as the solar kinematic phase, Δ_{21}, changes from $0(\text{mod}\pi)$ to $\pi/2(\text{mod}\pi)$. This amplitude modulation is the beat discussed in the previous section.

The phase $\phi_\odot$ in Eq. (5) depends only on solar parameters, Δ_{21} and θ_{12}, and is given as

$$
\begin{aligned}
\sin\phi_\odot &= \frac{c_{12}^2 \sin(2s_{12}^2\Delta_{21}) - s_{12}^2 \sin(2c_{12}^2\Delta_{21})}{\sqrt{1 - \sin^2 2\theta_{12}\sin^2\Delta_{21}}}, \\
\cos\phi_\odot &= \frac{c_{12}^2 \cos(2s_{12}^2\Delta_{21}) + s_{12}^2 \cos(2c_{12}^2\Delta_{21})}{\sqrt{1 - \sin^2 2\theta_{12}\sin^2\Delta_{21}}},
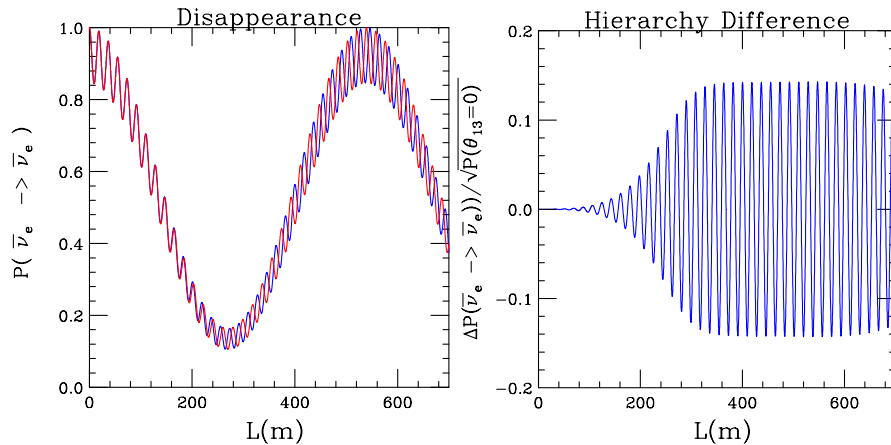\end{aligned} \quad (6)
$$

FIG. 1 (color online). In the left panel, antineutrino survival probability $P(\bar{\nu}_e \rightarrow \bar{\nu}_e)$ is plotted as a function of L. The blue (advanced) and the red (retarded) curves are for the normal and the inverted mass hierarchies, respectively. In the right panel, $\Delta P/\sqrt{P(\theta_{13} = 0)}$, which is defined in the text, is shown. Here the neutrino energy was fixed to 18.6 keV. This choice comes from the experiment we will discuss later in this paper.
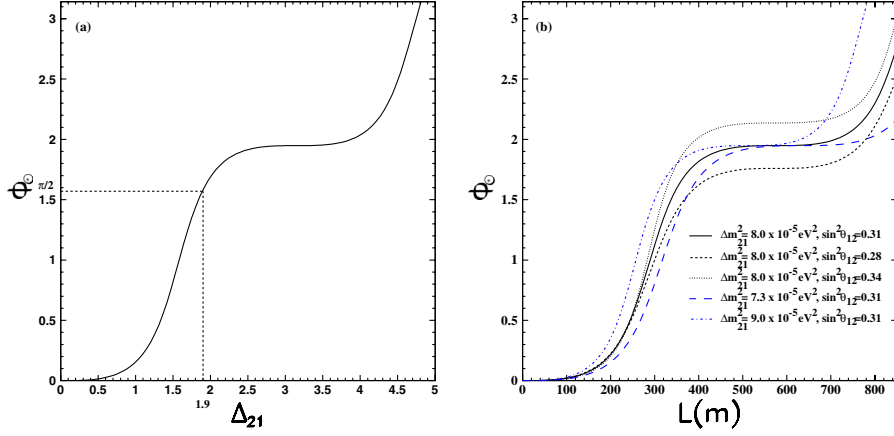
FIG. 2 (color online). (a) $\phi_\odot$ as a function of Δ_{21}. $\phi_\odot = \pi/2$ when $\Delta_{21} \approx 1.9$. (b) $\phi_\odot$ as a function of L for various choices of the solar parameters within the current allowed region. $\phi_\odot \approx \pi/2$ at about 350 m somewhat independent of the precise values for the solar parameters.

or, alternatively,

$$\phi_\odot = \arctan(\cos 2\theta_{12} \tan\Delta_{21}) - \Delta_{21} \cos 2\theta_{12}. \quad (7)$$

However, Eq. (6) contains quadrant information not available in Eq. (7). In Fig. 2, we show $\phi_\odot$ as a function of Δ_{21}. Note that it is an odd, monotonically increasing function of Δ_{21}.

Because of the monotonically increasing nature of $\phi_\odot$ and the $\pm$ sign in front of $\phi_\odot$, in Eq. (5), for the normal hierarchy the high frequency wiggles undergo a phase advancement as the wave evolves, whereas for the inverted hierarchy there is a phase retardation.[1] It is easy to show that

$$\phi_\odot(\Delta_{21} + \pi) = \phi_\odot(\Delta_{21}) + 2\pi\sin^2\theta_{12}, \quad (8)$$

i.e. the phase advancement (normal) or retardation (inverted) is $2\pi\sin^2\theta_{12}$ for every π increase of Δ_{21}. Equations (5) and (6) are the foundations of our investigation.

Some important observations are worth emphasizing immediately:
(i) Only Δ_{ee} varies at the atmospheric scale. Everything else, including phase $\phi_\odot$, varies at the solar scale. This is a useful distinction because these two scales differ by a factor of ~ 30.
(ii) The difference between probabilities corresponding to the two hierarchies (3) is given by

$$\frac{\Delta P}{\sqrt{P(\theta_{13} = 0)}} = \sin^2 2\theta_{13} \sin 2\Delta_{ee} \sin\phi_\odot, \quad (9)$$

to leading order in θ_{13}. ΔP becomes visible when the phase $\phi_\odot$ develops to order unity. From Fig. 2 this occurs at around the first solar oscillation maximum

$(\Delta_{21} = \pi/2)$ in agreement with the features exhibited in Fig. 1. From (9) we also see that the normal and the inverted hierarchies are maximally out of phase when $\phi_\odot = \pi/2$. This occurs when

$$\cot\Delta_{21} \cot(\Delta_{21} \cos 2\theta_{12}) = -\cos 2\theta_{12}. \quad (10)$$

The approximate solution to this equation, for θ_{12} around 30 degrees, is $\Delta_{21} \approx \frac{\pi}{2} + \cos 2\theta_{12}/(\pi\sin^2\theta_{12})$. For $\sin^2\theta_{12} = 0.31$, Eq. (10) is satisfied when $\Delta_{21} \approx 1.9$, i.e., just beyond the first solar oscillation maximum.
(iii) We notice that by doing transformation $\theta_{12} \to \pi/2 - \theta_{12}$ (or $s_{12} \leftrightarrow c_{12}$) in (6) flips the sign of $\phi_\odot$. It means that the mass hierarchy is confused by the presence of the particular type of *CPT* violation, the subtle one discussed in [20]. It occurs because we use the antineutrino channel; If we are able to use the neutrino channel, the problem of confusion does not arise because we know that $\theta_{12} < \pi/4$ from the solar neutrino observation.

B. Experimental strategy and requirements to the accuracy of measurement

We now describe our experimental strategy for determining the hierarchy. First, one needs to make a very precise measurement of Δm_{ee}^2 at short distances from the source, at around half the atmospheric oscillation length $L_0/2$, where

$$L_0 \equiv \frac{4\pi E}{\Delta m_{ee}^2} = 18.4\left[\frac{E}{18.6 \text{ keV}}\right]\left[\frac{\Delta m_{ee}^2}{2.5 \times 10^{-3} \text{ eV}^2}\right]^{-1} \text{m}. \quad (11)$$

Then, one must determine the sign in front of $\phi_\odot$ where the phase difference between normal and inverted hierarchy is maximal, i.e. $\Delta_{21} \approx 2$ as can be seen in Fig. 2. With

---

[1]Equivalently, one could interpret this phenomena as a change in the instantaneous effective Δm_{atm}^2. This interpretation is explored in Appendix A.

$\Delta_{ee}/\Delta_{21} \simeq 30$, it can be translated into the distance $L \approx [(2 \times 30)/\pi]L_0 \simeq 20L_0$ away from the source.

How well do we need to know Δm_{ee}^2? If we do not know the value of Δm_{ee}^2 with sufficient precision, one can adjust Δm_{ee}^2, depending upon the normal (NH) and the inverted (IH) hierarchies, so that the relation

$$2\Delta_{ee}|_{NH} + \phi_\odot = 2\Delta_{ee}|_{IH} - \phi_\odot \qquad (12)$$

holds at some L/E. Then, from Eq. (5) the hierarchy is completely confused as we will explicitly see in Sec. III A. It can be translated into

$$\frac{\Delta m_{ee}^2|_{IH} - \Delta m_{ee}^2|_{NH}}{\Delta m_{ee}^2}\left(\frac{\pi L}{L_0}\right) = \phi_\odot \qquad (13)$$

which leads to the requirement for the accuracy of measurement of Δm_{ee}^2 as $\delta(\Delta m_{ee}^2)/\Delta m_{ee}^2 \lesssim 2L_0/\pi L \simeq 3\%$. This is the critical value at which the hierarchy is completely confused, and if we want to do better, e.g., at least a factor of 3 times better than 3%, the first requirement is $\simeq$ 1% measurement of Δm_{ee}^2.

At this point the astute reader will be concerned that we are attempting to determine an oscillation phase after 20 or so oscillations. Are not the atmospheric oscillations completely washed out long before 20 L_0? To observe atmospheric oscillations 20 or so oscillations out, assuming coherence, demands that we can determine L/E per event to high precision. Figure 3 shows how the oscillations are reduced as the resolution on L/E is increased and that a precision better than 1% is required to see oscillation at ~20 oscillation lengths from the source.

In summary, to measure the sign of the phase and determine the hierarchy we have *two* important initial requirements:

  (i) The resolution on Δm_{ee}^2 measured in a short baseline experiment ($\sim L_0/2$ from the source) must be $\simeq 1\%$ or less.

 (ii) The resolution on L/E for the long-baseline experiment ($\sim 20 L_0$ from the source) must be $\simeq 1\%$ or less.

Usually, the neutrino energy cannot be determined experimentally with this accuracy, therefore, these preconditions are very difficult to meet, if not impossible.

C. Mass hierarchy reversal and comments on the reactor neutrino method

We have emphasized in the foregoing discussions the importance of identifying the quantity to be held fixed to define the mass hierarchy reversal, and proposed Δm_{ee}^2 as the solution. In this subsection, we want to elaborate this point and clarify how the difference between the normal and the inverted hierarchies can be made artificially larger by choosing different variables to define the hierarchy reversal.

In Fig. 4, presented is the survival probability of electron antineutrinos at a baseline of 50 km from a source which is averaged over the uncertainty of energy $3\%/\sqrt{E/\text{MeV}}$ as a function of neutrino energy E. It is shown in the left panel of Fig. 4 that, if we hold $|\Delta m_{32}^2|$ fixed in reversing the hierarchy from the normal to the inverted (as was done in [11]), the difference between the normal and the inverted hierarchies is clearly visible. However, the obvious distinction seen in the left panel of Fig. 4 disappears if we use Δm_{ee}^2 to hold when switching between the hierarchies as shown in the middle panel of Fig. 4. A simple explanation for such a marked difference is that, by holding $|\Delta m_{32}^2|$ fixed in reversing the hierarchy from the normal to the inverted, one maps the neutrino mass spectrum into a significantly different one, $|\Delta m_{31}^2|_{IH} = |\Delta m_{31}^2|_{NH} - 2\Delta m_{21}^2$. (See Appendix A for more about it.) This artificially enhances the difference between the hierarchies, as demonstrated in Fig. 4.

Despite that there exist some discrepancies at energies around 4 MeV, a peak energy of signal events in reactor experiments, the two disappearance probabilities can be made very close to each other over the energy range of 4 to 6 MeV if we allow the value of Δm_{ee}^2 for the inverted hierarchy to increase by 0.6% relative to the value for the
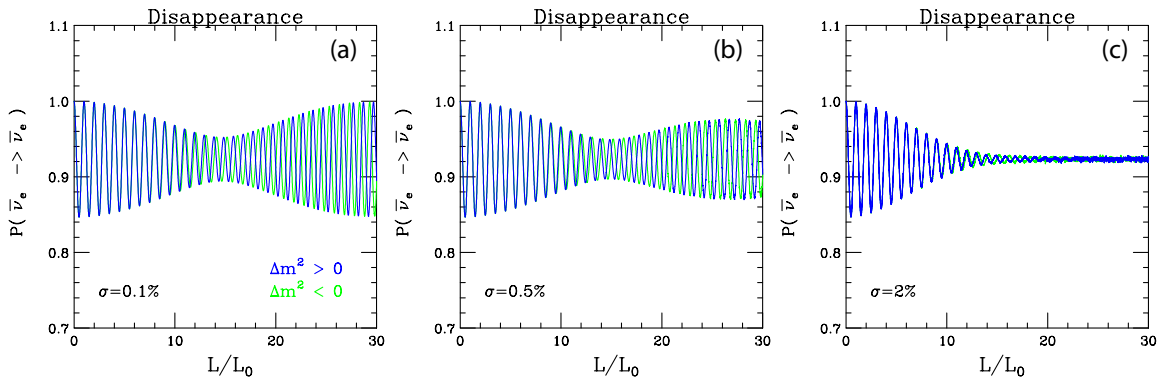

FIG. 3 (color online). The averaged $P(\nu_e \to \nu_e)$ versus distance measured in number of oscillation lengths, L_0. To help with visualization $P_\odot = \sin^2 2\theta_{12}\cos^4\theta_{13}\sin^2\Delta_{21}$ has been set to zero for these figures. (a) 0.1% Gaussian resolution on L/E. (b) 0.5% resolution on L/E. (c) 2% resolution on L/E. In (b) the oscillations are reduced at 20 or so oscillations out, but still observable; whereas in (c) the oscillations are averaged out by 15 L_0.
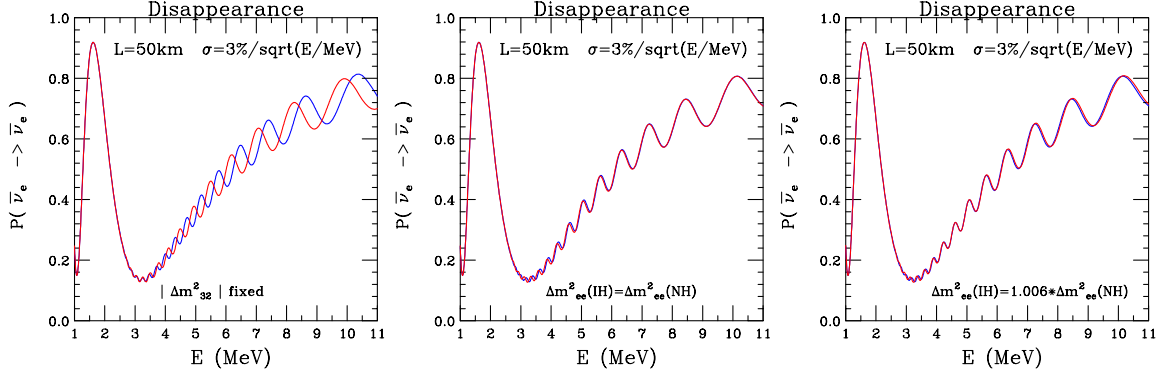
FIG. 4 (color online).   The $\bar{\nu}_e$ disappearance probability at 50 km from a reactor source as a function of the neutrino energy. The resolution on the energy is assumed to be $3\%/\sqrt{E/\text{MeV}}$. The blue (light gray) and the red (dark gray) curves are for the normal and the inverted mass hierarchies, respectively. In the left panel $|\Delta m^2_{32}|$ is held fixed when the hierarchy is flipped, whereas in the middle panel Δm^2_{ee} is held fixed. In the right panel Δm^2_{ee} for the inverted hierarchy is 0.6% larger than for the normal hierarchy.

normal hierarchy, as can be seen in the right panel of Fig. 4. The lesson we have learned from this exercise is that, unless we know Δm^2_{ee} to a subpercent level, the hierarchy can be easily confused by a tiny shift of the atmospheric Δm^2.

One might want to use neutrinos from reactors to determine the mass hierarchy by the present method, as suggested by the authors of [11]. However, the experimental requirements are very severe in order for this method to work. We believe that the three points discussed above deserve attention if one want to make a reliable estimate of sensitivity to the mass hierarchy resolution with reactor neutrinos: (1) definition of hierarchy reversal; (2) implementation of realistic energy resolution; and (3) robustness of the sensitivity to mass hierarchy resolution against the uncertainty of Δm^2_{ee}.

The recent Hanohano proposal [12] sidesteps some of these requirements by using a sophisticated Fourier transform technique. Detailed analysis around the atmospheric peak in Fourier space can tell us whether $|\Delta m^2_{32}|$ is greater or smaller than $|\Delta m^2_{31}|$, thus determining the hierarchy. There is no need to explicitly deal with the definition of hierarchy reversal. In this way, the two curves shown in the two right panels of Fig. 4 can, in principle, be distinguished. If this can be achieved in a realistic setting of the experiment, it represents a remarkable advance for reactor neutrino experiments, demonstrating the power of the Fourier transform technique.

III. EXPERIMENTAL SETUP, ANALYSIS METHOD, AND RESULTS

Most probably, the unique possibility to satisfy both requirements of the previous section is to make use of monochromatic beam from the bound-state beta decay $^3\text{H} \rightarrow {}^3\text{He} + \text{orbital } e^- + \bar{\nu}_e$ and detect it by the time-reversed resonant absorption reaction $\bar{\nu}_e + {}^3\text{He} + \text{orbital } e^- \rightarrow {}^3\text{H}$, the idea recently revived by Raghavan

[14]. For the Mössbauer enhancement to work, the method requires $\Delta E/E$ better than 10^{-16}, a truly monochromatic neutrino beam of 18.6 keV. Thus, the energy spread of the beam in such an experiment is automatically much narrower than what is required.

Having monochromaticity satisfied, the remaining requirement is on the baseline L. The short- and long-baseline measurements are to be done at the distances of ~ 10 m and $20L_0 \sim 350$ m from the source, respectively. Then, the requirement on $\Delta L/L$ of, say, 0.3% implies that the size of the source and the target must be limited, respectively, to ~ 3 cm and ~ 1 m in short- and long-baseline measurements. The former places severe limits on the sizes of the source and the detector. Assuming this requirement can be met, it has been shown by analyses with several concrete settings that a sensitivity to Δm^2_{ee} of $\simeq 0.3(\sin^2 2\theta_{13}/0.1)^{-1}\%$ at 1σ C.L. is possible [17]. Therefore, the first requirement listed in Sec. II B can be met if $\sin^2 2\theta_{13} \gtrsim 0.05$.

A. Experimental setup and how two-stage measurement works

We consider a possible experimental setup for determination of the neutrino mass hierarchy based on a Mössbauer enhanced $\bar{\nu}_e$ absorption experiment [14]. By using the revised estimate of the cross section $\sigma_{\text{res}} = 0.3 \times 10^{-32}$ cm^2 [14], the event rate is given by

$$R_{\text{enhanced}} = 3 \times 10^5 \left(\frac{S \cdot M_T}{1 \text{ MCi} \cdot 100 \text{ g}} \right) \left(\frac{L}{10 \text{ m}} \right)^{-2} \text{ day}^{-1}.$$

(14)

Therefore, one obtains about 1×10^6 (2500) events per 3 days (10 days) for 1 MCi source and 100 g ^{3}He target at a baseline distance $L = 10$ (350) m. The experiment should be done in two stages: In the first stage, Δm^2_{ee} and $\sin^2 2\theta_{13}$ should be determined very precisely by a measurement at baseline around ~ 10 m as demonstrated in [17]. We thus
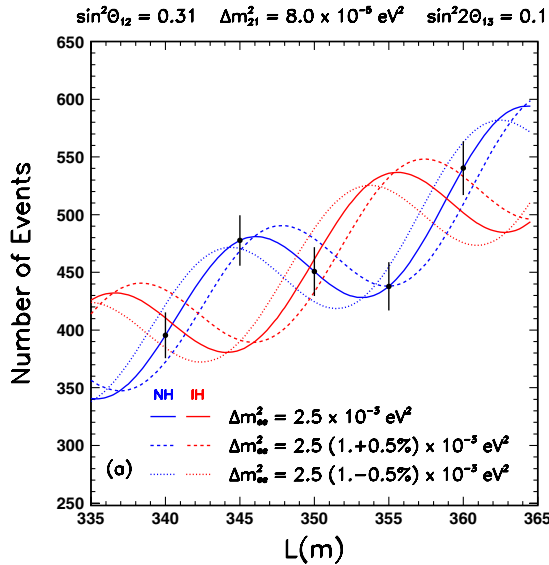
FIG. 5 (color online). Plotted are the expected number of events to be collected by detectors placed at the distances 340, 345, 350, 355, and 360 m from the source for $\Delta m_{ee}^2 = 2.5 \times 10^{-3}$ eV^2 and $\sin^2 2\theta_{13} = 0.1$ for the normal hierarchy, indicated by solid circles with error bars. Here $P_\odot$ is included (solar parameters are fixed to their best fit values). The expected number of events in the absence of oscillation is assumed to be 2000 at each detector position. The blue (light gray) solid curve which passes through the data points indicates a theoretical expectation assuming the normal hierarchy with $\Delta m_{ee}^2 = 2.5 \times 10^{-3}$ eV^2 and $\sin^2 2\theta_{13} = 0.1$, whereas the red (dark gray) curve off the data points is the one of inverted hierarchy with the same values of Δm_{ee}^2 and θ_{13}. Assuming that Δm_{ee}^2 is known to $\pm 0.5\%$ precision, the thick-dotted (thin-dotted) lines above and below the solid lines are the expectations with Δm_{ee}^2 0.5% above (below) that value.

do not discuss it further by just assuming the setting with 10 location measurements called the run IIB in [17]. For the second stage, we examine the setting with detectors placed at five locations $L = 350 \pm (0, 5, 10)$ m from the source, which covers a complete atmospheric oscillation length. The results of these two stages should be combined as we will discuss below.

In Fig. 5 we present the expected number of events for $\Delta m_{ee}^2 = 2.5 \times 10^{-3}$ eV^2 and $\sin^2 2\theta_{13} = 0.1$ at 5 locations mentioned above for the normal hierarchy, for 2000 events at each detector location in the absence of oscillation, which correspond to an exposure of about 20 MCi·g·day.[2] Throughout our analysis except for that in Sec. IV, we fix the solar parameters to their best fit values as $\sin^2 \theta_{12} = 0.31$ and $\Delta m_{21}^2 = 8.0 \times 10^{-5}$ eV^2.

---

[2]In view of Fig. 5, one may think that measurement at least 3 different baseline distances would be enough to detect relative phases of the beat and the wiggle around it. Though it is true, it turned out that the five point measurement can achieve better accuracy than the three point measurement for an equal total number of events.

and do not try to vary them. Δm_{ee}^2 is taken with a tentative expectation for its accuracy, $\Delta m_{ee}^2 = 2.5 \times 10^{-3}(1 \pm 0.5\%)$ eV^2. The case of the normal and the inverted hierarchy are plotted by the blue (light gray) and the red (dark gray) curves, respectively. It appears that, if enough statistics is accumulated and Δm_{ee}^2 is separately measured accurately, the five point measurement can discriminate between the normal and the inverted hierarchies. The details of the statistical procedure are described in the next subsection.

We show in three panels in Fig. 6 the allowed regions in the $\sin^2 2\theta_{13} - \Delta m_{ee}^2$ space obtained by the first stage alone (upper panels), by the second stage alone (middle panels), and the one obtained when the first and the second stages are combined (lower panels). The input parameters are taken as $\sin^2 2\theta_{13} = 0.1$, $\Delta m_{ee}^2 = 2.5 \times 10^{-3}$ eV^2, and the mass hierarchy is assumed to be the normal one. In the first-stage measurement to be done at around the distance $L_0/2 \simeq 10$ m from the source, $\sin^2 2\theta_{13}$ as well as Δm_{ee}^2 can be determined rather precisely. But, there is no
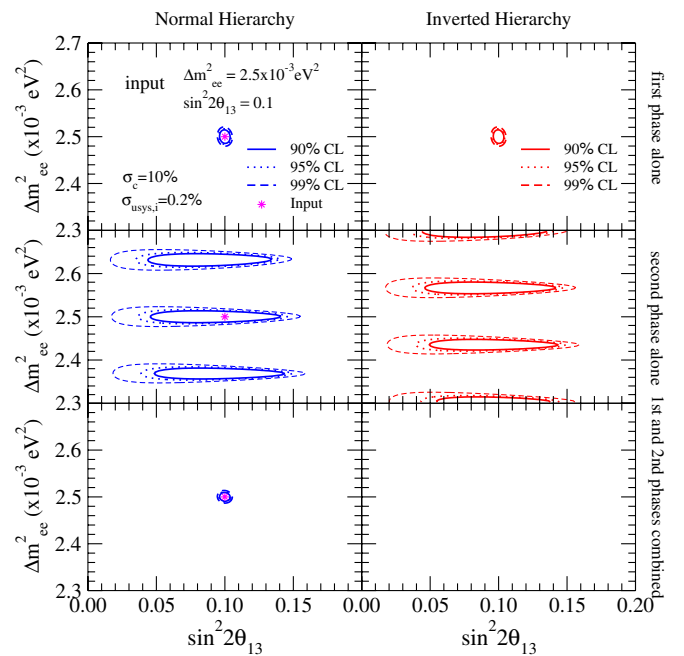

FIG. 6 (color online). The allowed regions in the $\sin^2 2\theta_{13} - \Delta m_{ee}^2$ plane obtained by the first stage alone (upper panels), the second stage alone (middle panels), and the combined result of these two stages (lower panels) for the case where the input parameters are $\sin^2 2\theta_{13} = 0.1$, $\Delta m_{ee}^2 = 2.5 \times 10^{-3}$ eV^2 with the normal hierarchy, based on the χ^2 analysis described in Sec. III B. The solar parameters are fixed to their current best fit values. The first stage is assumed to be performed at 10 positions at around $L \sim 9$ m following the run IIB in [17], whereas the second stage is assumed to be performed at 5 locations at $L = 350 \pm (0, 5, 10)$ m from the source. The three closed curves (red, blue, green) from inner to outer denote the ones obtained at 90% C.L., 95% C.L., and 99% C.L.

sensitivity to the mass hierarchy because the baseline is too short, as is the case of the reactor θ_{13} experiment.

The feature of the second-stage experiment presented in the middle panels of Fig. 6 requires some explanations. First of all, there exist many isolated islandlike allowed regions. Suppose that θ_{13} is given from some other experiments. Then, due to the cosine term in Eq. (5), the measurement will give a periodic solution

$$\Delta m_{ee}'^2 \approx \Delta m_{ee}^2 + \frac{4n\pi E}{L}, \qquad (n = \pm 1, \pm 2, \ldots) \quad (15)$$

for both of the hierarchies. If we take approximation $\phi_\odot = \pi/2$, there is a shift $2\pi E/L$ between the adjacent Δm_{ee}^2 solutions for the normal and the inverted hierarchies. Hence, the solutions of Δm_{ee}^2 are alternating in the normal and the inverted hierarchies with a constant shift $2\pi E/L$ between the adjacent solutions, the feature clearly visible in the middle panels of Fig. 6. The contours have finite widths, though prolonged, along the $\sin^2 2\theta_{13}$ direction because the second-stage measurement alone can determine θ_{13} but only with a limited accuracy.

It is clear that the second stage alone cannot determine either the value of Δm_{ee}^2 or the mass hierarchy. However, once the results of the first and the second stages are combined all the fake solutions are eliminated, as demonstrated in the lower panels of Fig. 6. It is evident that Δm_{ee}^2 must be determined with high accuracy in the first-stage measurement.

B. Analysis method and definition of χ^2

Now we give details of our analysis method. To calculate the sensitivity of the determination of the neutrino mass hierarchy by the first and second stages of the experiment combined, we compute

$$\Delta\chi^2_{\min}(\sin^2 2\theta_{13}) = \chi^2_{\min}(\text{wrong hierarchy})$$
$$- \chi^2_{\min}(\text{true hierarchy}), \quad (16)$$

where $\chi^2_{\min}(\text{true/wrong hierarchy})$ is the minimum of

$$\chi^2(\text{true/wrong hierarchy}) = \chi^2_1$$
$$+ \chi^2_2(\text{true/wrong hierarchy}), \quad (17)$$

with the first stage χ^2 given by

$$\chi^2_{1st}(\Delta m_{ee}^2, \sin^2 2\theta_{13}) = \sum_{i,j=1}^{10} \left[\frac{N_i^{1\text{-obs}} - N_i^{1\text{-theo}}}{N_i^{1\text{-theo}}} \right] (V_1^{-1})_{ij}$$
$$\times \left[\frac{N_j^{1\text{-obs}} - N_j^{1\text{-theo}}}{N_j^{1\text{-theo}}} \right], \quad (18)$$

and the second stage χ^2 given by

$$\chi^2_{2nd}(\Delta m_{ee}^2, \sin^2 2\theta_{13}, \text{sign}(\Delta m_{31}^2))$$
$$= \sum_{i,j=1}^{5} \left[\frac{N_i^{2\text{-obs}} - N_i^{2\text{-theo}}}{N_i^{2\text{-theo}}} \right] (V_{2\text{-obs}}^{-1})_{ij} \left[\frac{(N_j^2 - N_j^{2\text{-theo}})}{N_j^{2\text{-theo}}} \right].$$
$$(19)$$

$N_i^{1,2\text{-obs}}$ is the number of events at baseline L_i for a given input hierarchy and values of the mixing parameters (observed events), while $N_i^{1,2\text{-theo}}$ is the theoretically expected number of events at baseline L_i for a given set of oscillation parameters. We use, as in Ref. [17], the correlation matrices

$$(V_{1,2}^{-1})_{ij} = \frac{\delta_{ij}}{\sigma_{ui}^2} - \frac{1}{\sigma_{ui}^2\sigma_{uj}^2} \frac{\sigma_c^2}{[1 + (\sum_k \frac{1}{\sigma_{uk}^2})\sigma_c^2]}, \quad (20)$$

where $\sigma_{ui}^2 = \sigma_{usys}^2 + 1/N_i^{1,2\text{-th}}$.

The estimation of the uncorrelated systematic uncertainty is the key issue in our sensitivity analysis. In [17] two cases of the error, $\sigma_{usys} = 0.2\%$ and 1%, are examined. The former corresponds to the case of movable detector, assuming that a direct extraction or real-time detection of produced ^{3}H atom is possible. The latter is a tentative estimate for the case of multiple identical detectors. We use the correlated systematic uncertainty $\sigma_c = 10\%$, though the results are insensitive to σ_c. We adopt the same numbers as these for the uncertainties in our analysis for both the first and the second stages of the experiment.

In our χ^2 analysis, for simplicity, the solar mixing parameters are fixed to the current best fit values, ignoring their uncertainties. Therefore, the fitting parameters are Δm_{ee}^2, $\sin^2 2\theta_{13}$, and the sign of Δm_{31}^2. Note, however, that χ^2_{1st} for the first stage has practically no dependence on solar parameters as well as the mass hierarchy due to too short baseline. The current uncertainty on the values of the solar parameter are not so relevant for the determination for the hierarchy because $\phi_\odot$ does not depend strongly on them [see Fig. 2(b)] as pointed out previously.

C. Sensitivity to mass hierarchy determination

Now, we present our estimation of the sensitivity of the two-stage Mössbauer $\bar{\nu}_e$ experiment to the determination of the neutrino mass hierarchy. In Fig. 7 we present the region of sensitivity to resolving the mass hierarchy at 90%, 95%, and 99% C.L., denoted by the black solid, the red dashed, and the blue dotted curves, respectively. The abscissa is $\sin^2 2\theta_{13}$ and the ordinate is the number of events per detector in the long-baseline experiment. Here, 90%, 95%, and 99% C.L. correspond to $\Delta\chi^2_{\min} = \chi^2_{\min}(\text{wrong hierarchy}) - \chi^2_{\min}(\text{true hierarchy}) = 2.71$, 3.84, and 6.63, respectively. Left and right panels are for the cases where the uncorrelated systematic uncertainty is 0.2% and 1%, respectively.

Assuming $\sigma_{usys} = 0.2\%$, we can see that the hierarchy can be determined at 90% (99%) C.L. for $\sin^2 2\theta_{13}$ down to
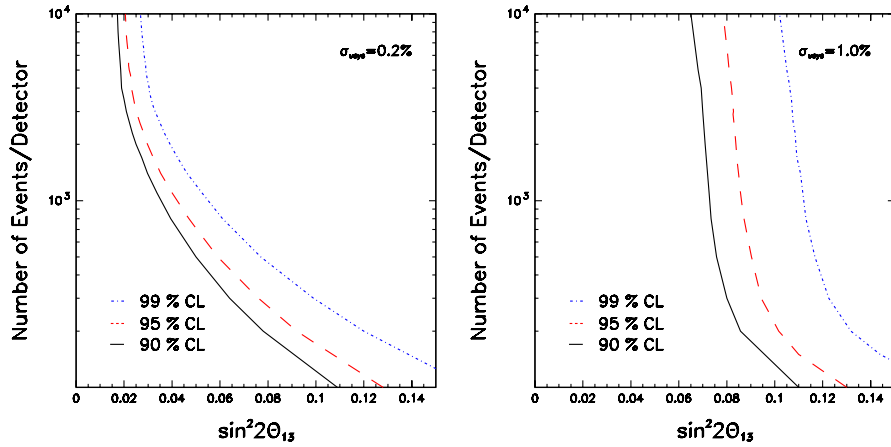
FIG. 7 (color online).   The region of sensitivity to resolving the mass hierarchy in $\sin^2 2\theta_{13}$-event number (per detector) space. The black solid, the red dashed, and the blue dotted curves denote the region boundary at 90%, 95%, and 99% C.L., respectively. The left and right panels are for the cases of uncorrelated systematic uncertainties of 0.2% and 1%, respectively.

0.035 (0.06) for 1000 events and down to 0.025 (0.04) for 2000 events. For a larger error $\sigma_{\text{usys}} = 1\%$, the critical value of $\sin^2 2\theta_{13}$ will be ~ 0.08 (0.11) at 90% (99%) C.L. approximately independent of the number of events larger than ~ 1000. This is caused by the fact that the precision on the determination of Δm_{ee}^2 at the first stage is highly dependent on this systematic uncertainty [17].

IV. DETERMINATION OF THE SOLAR PARAMETERS

In the second stage of the Mössbauer experiment, the detectors are placed just after the first solar oscillation maximum in order to determine the mass hierarchy, as we discussed in the previous section. In a possible third stage of the experiment, one could envisage moving the detectors somewhat closer to the source in order to cover the region around this maximum. It will allow us a precise determination of the solar-scale oscillation parameters, Δm_{21}^2 and θ_{12}.

In order to optimize the determination of these parameters, we assume that the measurements will be performed at the following 10 different detector locations:

$$L_n = [200 + 50(n - 1)] \text{ m}, \tag{21a}$$

$$L_n' = L_n - L_0/2, \qquad n = 1, 2, \ldots, 5. \tag{21b}$$

First, in order to observe the oscillation driven by the solar Δm_{21}^2, we consider the configuration of 5 detector locations (L_n) separated by 50 m, ranging from 200 m to 400 m as in Eq. (21a). In this way, we can cover the whole range of solar-scale oscillation before and after the dip due to the oscillation maximum (see Fig. 1). Second, in order to minimize the unwanted effect due to the rapid oscillations driven by the atmospheric Δm_{ee}^2, we have to place, for each location L_n, another detector (or move detector to another location) at L_n' separated from L_n by half the atmospheric oscillation length, $L_0/2$. See Eq. (21b). The setting of five

pairs of detector locations works because the average of the oscillation probabilities corresponding to these two positions L_n and L_n' is, at first approximation, independent of θ_{13} and Δm_{ee}^2 and thus is free from any ambiguity associated with the atmospheric oscillations.

In this calculation we assume that the exposure is such that the same number of events (1000) in the absence of oscillation are collected at each detector location. We take the pessimistic value of the systematic uncertainty $\sigma_{\text{usys}} = 1\%$ instead of 0.2% because the results do not differ much: The sensitivity is still dominated by the statistics in this regime. As in the previous sections, the input values of the other oscillation parameters are fixed as $\Delta m_{\text{ee}}^2 = 2.5 \times 10^{-3} \text{ eV}^2$, $\sin^2 \theta_{12} = 0.31$, and $\Delta m_{21}^2 = 8.0 \times 10^{-5} \text{ eV}^2$.

In Fig. 8 we show how well Δm_{21}^2 and $\sin^2 \theta_{12}$ can be determined by this experiment. The obtained sensitivity contours with $\sin^2 \theta_{13} = 0$ are presented by the green lines (which practically overlapped with the black ones) in Fig. 8. From this result, we conclude that the precision one can achieve for $\sin^2 \theta_{12}$ is about 1.6% (4.0%) at 68.27% (99.73%) C.L. for 2 DOF whereas that for Δm_{21}^2 is about 0.9% (2.2%) at 68.27% (99.73%) C.L. for 2 DOF. Comparing this result with the sensitivity which can be achieved by the dedicated reactor experiment for the similar number of events studied in Ref. [21], the precision we obtained for $\sin^2 \theta_{12}$ and Δm_{21}^2 in this work are comparable or better, in particular, for Δm_{21}^2 (see e.g. Fig. 5 of the first article in [21]).

In the above argument, we have assumed that L_0 (or Δm_{ee}^2) can be determined very precisely in the first stage of the experiment allowing us to place the detector pair separated exactly by $L_0/2$. In reality, however, the determination of L_0 will always carry some uncertainties. Moreover, if $\sin^2 2\theta_{13}$ is too small or the uncorrelated systematic uncertainty (σ_{usys}) is not small enough, the neutrino mass hierarchy will not be determined in the
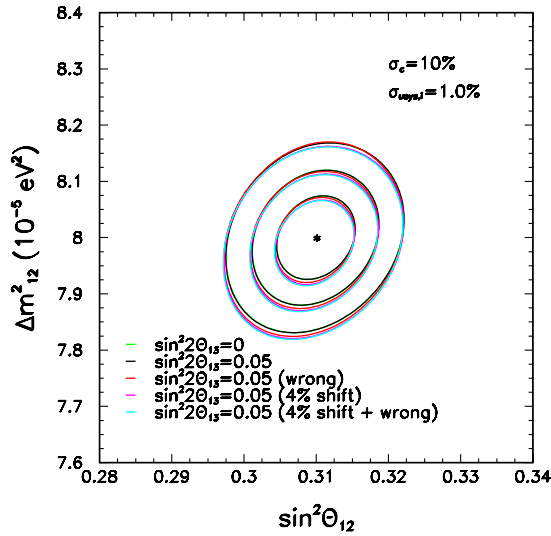
FIG. 8 (color online). Expected allowed regions in the plane $\sin^2\theta_{12} - \Delta m^2_{21}$ for 1000 events taken at each detector position at 68.27% (inner curves), 95.0% (middle curves), and 99.73% (outer curves) C.L. for 2 DOF. We assumed the measurement will be done at 10 different detector locations, $L_n = [200 + 50(n-1)]$ m and $L'_n = L_n - L_0/2$ with $n = 1, 2, \ldots, 5$. The input values used are $\sin^2\theta_{12} = 0.31$, $\Delta m^2_{21} = 8.0 \times 10^{-5}$ eV^2, and $\Delta m^2_{ee} = 2.5 \times 10^{-3}$ eV^2. The green and black curves are for the input values of $\sin^2 2\theta_{13} = 0$ and 0.05, respectively. The other curves are also for $\sin^2 2\theta_{13} = 0.05$ but fitted with the wrong hierarchy (red), Δm^2_{ee} shifted by 4% (magenta) and the wrong hierarchy and Δm^2_{ee} shifted by 4% (cyan). Here we have supposed $\sigma_{usys} = 1\%$.

second stage. Then, the question is: What is the additional ambiguities that occur in determination of the solar oscillation parameters in the presence of these uncertainties? Fortunately, we can show that our choice of detector locations defined in Eqs. (21a) and (21b) guarantees that these uncertainties will not deteriorate the precision in the determination of the solar parameters.

In order to check the stability of the results against the uncertainties mentioned above, we performed a fit by assuming the incorrect mass hierarchy and/or slightly incorrect value of Δm^2_{ee} by shifting its value by 4%. The results are shown by the blue, the magenta, and the light blue curves in Fig. 8 where we can see that, for each C.L., all the curves are very close to each other, indicating that our results are quite stable against these uncertainties.

We also examine the stability of the sensitivities to possible nonzero values of θ_{13}. In Fig. 8 we show the sensitivity contours for the input values of $\sin^2 2\theta_{13} = 0.05$ (black curve) in comparison to that with $\sin^2 2\theta_{13} = 0.0$ (green curve). We note that these 2 curves are very close to each other implying that the effect of nonzero θ_{13} is quite small. We emphasize that this feature is in a marked contrast with any of the alternative methods for measuring θ_{12}, including the reactor [21] and the solar neutrino methods [22]. In these methods there is no way,
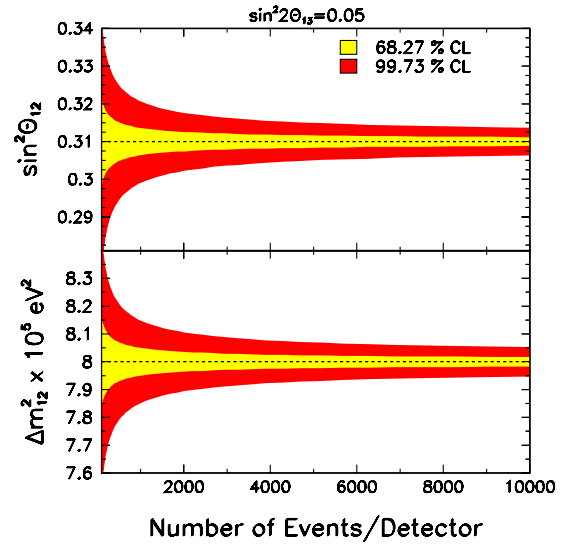

FIG. 9 (color online). Determination of $\sin^2\theta_{12}$ (upper panel) and Δm^2_{21} (lower panel) as a function of detector exposure at 68.27% and 99.73% C.L. for 1 DOF. Here $\sigma_{usys} = 1\%$. The dashed lines show the input values.

unless determined by some other experiments, to control the errors which come from nonzero θ_{13} [23], whereas in our present method, there is a built-in mechanism which eliminates the uncertainties that come from the atmospheric oscillation parameters, in particular, from θ_{13}.

In Fig. 9 we show how the precision for 1 DOF of each of the solar parameters improves with statistics, that is, as a function of the number of events that would be collected at each detector in the absence of oscillation. As in the previous plot, we have assumed that $\sigma_{usys} = 1\%$. We observe that until ~ 1000 events, the precision improves rapidly as the number of events increase, and then after the rapidness of the improvement become smaller. The ultimate precision which can be achieved in the limit of very large statistics with $\sim 10\,000$ events (per detector) for $\sigma_{usys} = 1\%$ would be $\sim 0.4\%$ (1.2%) for 68.27% (99.73%) C.L. for $\sin^2\theta_{12}$ and $\sim 0.2\%$ (0.7%) for 68.27% (99.73%) C.L. for Δm^2_{21}. Notice that measurement of Δm^2 to the accuracy of subpercent level is usually not possible because the absolute energy scale of leptons is hard to be determined at such accuracy, and it acts as a limiting factor for reducing the Δm^2 error [7]. In our case, monochromaticity of the $\bar\nu_e$ beam with known energy removes the necessity for such calibration for determining absolute energy scale.

V. CONCLUDING REMARKS

In this paper, we have shown that the neutrino mass hierarchy can be determined only by *a single experiment* based on resonant $\bar\nu_e$ absorption reaction enhanced by the Mössbauer effect. In its first stage, Δm^2_{ee} must be accurately determined by $L \sim 10$ m measurements. In the sec-

ond stage of the experiment, the relative phase of the atmospheric oscillation (wiggles) between the normal vs inverted mass hierarchies, phase advancement, or retardation must be discriminated by measurements at $L \sim 350$ m. It can be executed thanks to the ultramonochromatic nature of neutrino beam which would allow us to detect the relative phase of atmospheric oscillation even after 20 oscillations. We stress that the monochromaticity is special to the resonant $\bar{\nu}_e$ absorption reaction, most probably the unique experimental way to realize this principle.

We concluded that, assuming $\sigma_{\text{usys}} = 0.2\%$, the hierarchy can be determined at 90% (99%) C.L. for $\sin^2 2\theta_{13}$ down to 0.035 (0.06) for 1000 events collected at five different positions and down to 0.025 (0.04) for 2000 events. For a larger error $\sigma_{\text{usys}} = 1\%$, the critical value of $\sin^2 2\theta_{13}$ will be ~ 0.08 (0.11) at 90% (99%) C.L. approximately independent of the number of events for more than ~ 1000 events.

We have also shown that, in a third stage of the experiment, by positioning detectors in different locations, it is possible to determine the solar-scale parameters too. The precision one can achieve with 1000 events in each detector for $\sin^2 \theta_{21}$ is about 1.6% (4.0%) at 68.27% (99.73%) C.L. whereas that for Δm_{21}^2 is about 0.9% (2.2%) at 68.27% (99.73%) C.L., all for 2 DOF. The accuracies improve as data taking proceeds and the errors would reduce by a factor of $\simeq 3$ when an order of magnitude larger number of events is taken.

It is in fact remarkable that the experimental setup considered in this paper allows us to make a precise measurement of all the mixing parameters appear in the oscillation probability for $\nu_e \rightarrow \nu_e$ channel, θ_{12}, θ_{13}, Δm_{21}^2, Δm_{ee}^2 and the neutrino mass hierarchy only by a single experiment, independent of any other experiments. The only parameters inaccessible by the method are θ_{23} and the CP phase δ, but precision measurement of the other mixing parameters will certainly help in determining these parameters by other experiments.

Some remarks are in order:

(i) As noted in Sec. II A, our method of determining the mass hierarchy can be confused by the CPT violation of the type with θ_{12} in different octants in the neutrino and the antineutrino sectors. It in turn implies that, once the mass hierarchy is determined by some other means, the measurement we propose in this paper can be regarded as testing that particular type of CPT violation.

(ii) Because of the capability of resolving atmospheric wiggles even after 20 atmospheric oscillations away from the source, this experiment could be sensitive to other dynamics [24] which differ from the standard three flavor mass induced oscillation one. In particular, one can perhaps probe mechanisms such as neutrino decay [25], decoherence [26], mixing with

sterile neutrinos [27], violation of Lorentz invariance or the equivalence principle [28], long-range leptonic forces [29], and extra dimensions [30].

Finally, we emphasize that realizing the proposed Mössbauer $\bar{\nu}_e$ experiment is crucial in order to make all the discussions in this paper meaningful. The principle of the experiment is well formulated by having the decay producing source $\bar{\nu}_e$ and the absorption reaction in the target as T-conjugate channels with each other, allowing mutual cancellation of the large part of the atomic shift [14,31]. Nonetheless, it still remains unclear to what extent the ^{3}He atom in the target experiences exactly the same environment as the ^{3}H atom in the source [32]. This point has to be (and will be) investigated in a systematic way. If the experiment is indeed realizable, it will certainly open a new window for neutrino experiments which can explore the neutrino properties in an otherwise inaccessible manner.

APPENDIX A: THE EFFECTIVE ATMOSPHERIC Δm^2

The advancement or retardation of the phase, $\phi_\odot$, could be interpreted as a change in the effective atmospheric Δm^2. Such an effective atmospheric Δm^2, at L/E, is naturally defined by

$$\Delta m_{\text{eff}}^2(L/E) \equiv \frac{d(2\Delta_{\text{ee}} \pm \phi_\odot)}{d(L/2E)}$$

$$= \Delta m_{\text{ee}}^2$$

$$\pm \frac{1}{2} \Delta m_{21}^2 \cos 2\theta_{12} \frac{\sin^2 2\theta_{12} \sin^2 \Delta_{21}}{1 - \sin^2 2\theta_{12} \sin^2 \Delta_{21}}$$

$$= \left(\frac{c_{12}^2 - \frac{1}{2} \sin^2 2\theta_{12} \sin^2 \Delta_{21}}{1 - \sin^2 2\theta_{12} \sin^2 \Delta_{21}} \right) |\Delta m_{31}^2|$$

$$+ \left(\frac{s_{12}^2 - \frac{1}{2} \sin^2 2\theta_{12} \sin^2 \Delta_{21}}{1 - \sin^2 2\theta_{12} \sin^2 \Delta_{21}} \right) |\Delta m_{32}^2|,$$

$$(A1)$$

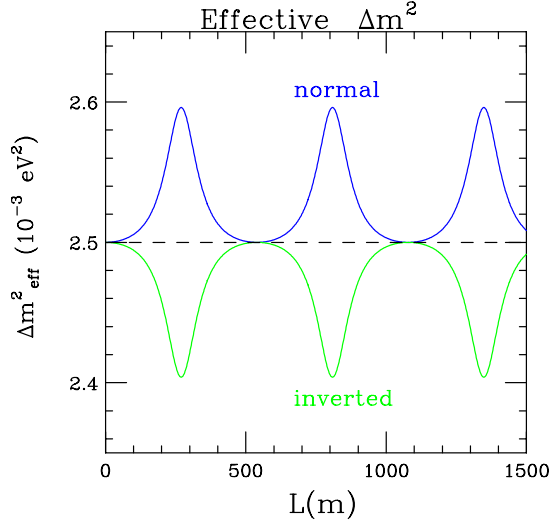where the positive (negative) sign, in Eq. (A1), is for the

FIG. 10 (color online). $\Delta m_{\mathrm{eff}}^2$ as a function of baseline at 18.6 keV neutrino energy for both the normal and inverted hierarchies. The dashed line is Δm_{ee}^2 which has been assumed to be the same for the normal and inverted hierarchies for this plot. In general, unless Δm_{ee}^2 is determined precisely it need not take exactly the same value for both hierarchies. The maximum difference between $\Delta m_{\mathrm{eff}}^2$ and Δm_{ee}^2 occurs at the solar oscillation maxima, i.e. when $\Delta_{21} = (2n - 1)\pi/2$.

normal (inverted) hierarchy. For $\Delta_{21} \ll 1$, we recover Δm_{ee}^2, since this is in essence its definition, see Ref. [6] for details. Thus Eq. (A1) is the generalization of Δm_{ee}^2 to arbitrary L/E. In Fig. 10 we show the variation of $\Delta m_{\mathrm{eff}}^2$ as a function of baseline for both the normal and inverted hierarchies. The extrema of the difference between $\Delta m_{\mathrm{eff}}^2(L/E)$ and Δm_{ee}^2 are given by

$$
\frac{1}{2} \Delta m_{21}^2 \cos 2\theta_{12} \frac{\sin^2 2\theta_{12} \sin^2 \Delta_{21}}{1 - \sin^2 2\theta_{12} \sin^2 \Delta_{21}}
$$
$$
= \begin{cases} 0 & \text{at } \Delta_{21} = n\pi \\ \frac{1}{2} \frac{\sin^2 2\theta_{12}}{\cos 2\theta_{12}} \Delta m_{21}^2 & \text{at } \Delta_{21} = (2n-1)\pi/2. \end{cases} \quad \text{(A2)}
$$

As the oscillations go through the solar maxima, the fractional increase (decrease) in the effective atmospheric Δm^2 is

$$
\frac{1}{2} \frac{\sin^2 2\theta_{12}}{\cos 2\theta_{12}} \frac{\Delta m_{21}^2}{\Delta m_{\mathrm{ee}}^2} \approx 4\%, \quad \text{(A3)}
$$

for the normal (inverted) hierarchy. It is the accumulated effect of this small difference in the effective atmospheric Δm^2 for the normal and inverted hierarchies that leads to the observable phase difference shown in Fig. 1. Since

$$
\frac{1}{2} \int_0^{L/E} d(L/E) \Delta m_{\mathrm{eff}}^2(L/E) = (2\Delta_{\mathrm{ee}} \pm \phi_\odot)|_{L/E}, \quad \text{(A4)}
$$

as it must.

APPENDIX B: ν_μ DISAPPEARANCE

For ν_μ disappearance in vacuum, most of the results of this paper can be applied, using the following translation:

$$
\sin^2\theta_{12} \Rightarrow \frac{|U_{\mu 2}|^2}{|U_{\mu 1}|^2 + |U_{\mu 2}|^2} \quad \text{and} \quad \sin^2\theta_{13} \Rightarrow |U_{\mu 3}|^2. \quad \text{(B1)}
$$

With this translation the atmospheric $\Delta m_{\mu\mu}^2$ and phase, $\phi_\odot^\mu$, are given by

$$
\Delta m_{\mu\mu}^2 \equiv \frac{|U_{\mu 1}|^2 |\Delta m_{31}^2| + |U_{\mu 2}|^2 |\Delta m_{32}^2|}{|U_{\mu 1}|^2 + |U_{\mu 1}|^2} \quad \text{(B2)}
$$

and

$$
\phi_\odot^\mu = \arctan\left(\frac{|U_{\mu 1}|^2 - |U_{\mu 2}|^2}{|U_{\mu 1}|^2 + |U_{\mu 2}|^2} \tan\Delta_{21} \right)
$$
$$
- \frac{|U_{\mu 1}|^2 - |U_{\mu 2}|^2}{|U_{\mu 1}|^2 + |U_{\mu 2}|^2} \Delta_{21}. \quad \text{(B3)}
$$

Then

$$
P(\nu_\mu \to \nu_\mu) = 1 - 4|U_{\mu 2}|^2 |U_{\mu 1}|^2 \sin^2 \Delta_{21}
$$
$$
- 2|U_{\mu 3}|^2 (1 - |U_{\mu 3}|^2)
$$
$$
\times \left[1 - \sqrt{1 - \frac{4|U_{\mu 1}|^2 |U_{\mu 2}|^2}{(|U_{\mu 1}|^2 + |U_{\mu 2}|^2)^2} \sin^2 \Delta_{21}} \right.
$$
$$
\left. \times \cos(2\Delta_{\mu\mu} \pm \phi_\odot^\mu) \right]. \quad \text{(B4)}
$$

Since numerically

$$
\frac{|U_{\mu 1}|^2 - |U_{\mu 2}|^2}{|U_{\mu 1}|^2 + |U_{\mu 2}|^2} \approx -\cos 2\theta_{12}, \quad \text{(B5)}
$$

the phase for ν_μ disappearance is approximately minus the phase for ν_e disappearance, i.e.

$$
\phi_\odot^\mu \approx -\phi_\odot^e. \quad \text{(B6)}
$$

Therefore the normal hierarchy is retarded while the inverted hierarchy is advanced. This is the opposite sign to what happens for ν_e disappearance but the rate of change is approximately the same.

The effective atmospheric Δm^2 for ν_μ disappearance at any L/E is given by

$$\Delta m_{\rm eff}^2(\mu\mu) = \left[\frac{|U_{\mu1}|^2(|U_{\mu1}|^2 + |U_{\mu2}|^2) - 2|U_{\mu1}|^2|U_{\mu2}|^2\sin^2\Delta_{21}}{(|U_{\mu1}|^2 + |U_{\mu2}|^2)^2 - 4|U_{\mu1}|^2|U_{\mu2}|^2\sin^2\Delta_{21}}\right]|\Delta m_{31}^2|$$

$$+ \left[\frac{|U_{\mu2}|^2(|U_{\mu1}|^2 + |U_{\mu2}|^2) - 2|U_{\mu1}|^2|U_{\mu2}|^2\sin^2\Delta_{21}}{(|U_{\mu1}|^2 + |U_{\mu2}|^2)^2 - 4|U_{\mu1}|^2|U_{\mu2}|^2\sin^2\Delta_{21}}\right]|\Delta m_{32}^2|. \tag{B7}$$

Again for small Δ_{21} this reduces to $\Delta m_{\mu\mu}^2$ given by Eq. (B2).

For ν_τ disappearance, just replace $|U_{\mu j}|^2$ with $|U_{\tau j}|^2$ in the equations of this Appendix.

---

[1] For a recent review, see R. N. Mohapatra and A. Y. Smirnov, Annu. Rev. Nucl. Part. Sci. **56**, 569 (2006).

[2] V. D. Barger, S. Geer, R. Raja, and K. Whisnant, Phys. Lett. B **485**, 379 (2000); A. Cervera, A. Donini, M. B. Gavela, J. J. Gomez Cadenas, P. Hernandez, O. Mena, and S. Rigolin, Nucl. Phys. **B579**, 17 (2000); **B593**, 731 (2001); H. Minakata and H. Nunokawa, J. High Energy Phys. 10 (2001) 001; P. Huber, M. Lindner, and W. Winter, Nucl. Phys. **B645**, 3 (2002); V. Barger, D. Marfatia, and K. Whisnant, Phys. Rev. D **65**, 073023 (2002); H. Minakata, H. Nunokawa, and S. J. Parke, Phys. Rev. D **68**, 013010 (2003); O. Mena and S. J. Parke, Phys. Rev. D **70**, 093011 (2004); O. Mena Requejo, S. Palomares-Ruiz, and S. Pascoli, Phys. Rev. D **72**, 053002 (2005); M. Ishitsuka, T. Kajita, H. Minakata, and H. Nunokawa, Phys. Rev. D **72**, 033003 (2005).

[3] D. Beavis *et al.*, arXiv:hep-ex/0205040; M. V. Diwan *et al.*, Phys. Rev. D **68**, 012002 (2003); V. Barger, M. Dierckxsens, M. Diwan, P. Huber, C. Lewis, D. Marfatia, and B. Viren, Phys. Rev. D **74**, 073004 (2006); R. Gandhi, P. Ghoshal, S. Goswami, P. Mehta, and S. Uma Sankar, Phys. Rev. D **73**, 053001 (2006).

[4] T. Kajita, Next Generation of Nucleon Decay and Neutrino Detectors (NNN05), Aussois, Savoie, France, 2005, http://nnn05.in2p3.fr/; S. Palomares-Ruiz and S. T. Petcov, Nucl. Phys. **B712**, 392 (2005); S. T. Petcov and T. Schwetz, Nucl. Phys. **B740**, 1 (2006); R. Gandhi, P. Ghoshal, S. Goswami, P. Mehta, and S. Uma Sankar, arXiv:hep-ph/0506145.

[5] A. de Gouvea, J. Jenkins, and B. Kayser, Phys. Rev. D **71**, 113009 (2005);

[6] H. Nunokawa, S. J. Parke, and R. Zukanovich Funchal, Phys. Rev. D **72**, 013009 (2005).

[7] H. Minakata, H. Nunokawa, S. J. Parke, and R. Zukanovich Funchal, Phys. Rev. D **74**, 053008 (2006).

[8] A. S. Dighe and A. Y. Smirnov, Phys. Rev. D **62**, 033007 (2000); H. Minakata and H. Nunokawa, Phys. Lett. B **504**, 301 (2001); C. Lunardini and A. Y. Smirnov, J. Cosmol. Astropart. Phys. 06 (2003) 009; V. Barger, P. Huber, and D. Marfatia, Phys. Lett. B **617**, 167 (2005).

[9] A. S. Dighe, M. T. Keil, and G. G. Raffelt, J. Cosmol. Astropart. Phys. 06 (2003) 005; 06 (2003) 006; R. Tomas, M. Kachelriess, G. Raffelt, A. Dighe, H. T. Janka, and L. Scheck, J. Cosmol. Astropart. Phys. 09 (2004) 015.

[10] S. Pascoli, S. T. Petcov, and T. Schwetz, Nucl. Phys. **B734**,

24 (2006); S. Choubey and W. Rodejohann, Phys. Rev. D **72**, 033016 (2005).

[11] S. T. Petcov and M. Piai, S. Choubey, S. T. Petcov, and M. Piai, Phys. Rev. D **68**, 113006 (2003).

[12] J. Learned, S. Dye, S. Pakvasa, and R. Svoboda, arXiv:hep-ex/0612022.

[13] L. A. Mikaelyan, B. G. Tsinoev, and A. A. Borovoi, Yad. Fiz. **6**, 349 (1967) [Sov. J. Nucl. Phys. **6**, 254 (1968)].

[14] R. S. Raghavan, arXiv:hep-ph/0601079.

[15] W. M. Visscher, Phys. Rev. **116**, 1581 (1959); W. P. Kells and J. P. Schiffer, Phys. Rev. C **28**, 2162 (1983).

[16] J. N. Bahcall, Phys. Rev. **124**, 495 (1961).

[17] H. Minakata and S. Uchinami, New J. Phys. **8**, 143 (2006).

[18] A. de Gouvea and W. Winter, Phys. Rev. D **73**, 033003 (2006).

[19] W. M. Yao *et al.* (Particle Data Group), J. Phys. G **33**, 1 (2006).

[20] A. de Gouvea and C. Pena-Garay, Phys. Rev. D **71**, 093002 (2005).

[21] H. Minakata, H. Nunokawa, W. J. C. Teves, and R. Zukanovich Funchal, Phys. Rev. D **71**, 013005 (2005); Nucl. Phys. B, Proc. Suppl. **145**, 45 (2005); A. Bandyopadhyay, S. Choubey, S. Goswami, and S. T. Petcov, Phys. Rev. D **72**, 033013 (2005); J. F. Kopp, M. Lindner, A. Merle, and M. Rolinec, J. High Energy Phys. 01 (2007) 053; S. T. Petcov and T. Schwetz, Phys. Lett. B **642**, 487 (2006).

[22] M. Nakahata, 5th Workshop on ''Neutrino Oscillations and their Origin'' (NOON2004), 2004, Odaiba, Tokyo, Japan, http://www-sk.icrr.u-tokyo.ac.jp/noon2004/.

[23] M. C. Gonzalez-Garcia and C. Peña-Garay, Phys. Lett. B **527**, 199 (2002).

[24] M. C. Gonzalez-Garcia and M. Maltoni, Phys. Rev. D **70**, 033010 (2004); R. Foot, C. N. Leung, and O. Yasuda, Phys. Lett. B **443**, 185 (1998).

[25] J. F. Beacom and N. F. Bell, Phys. Rev. D **65**, 113009 (2002).

[26] F. Benatti and R. Floreanini, J. High Energy Phys. 02 (2000) 032; F. Benatti and R. Floreanini, Phys. Rev. D **64**, 085015 (2001); A. M. Gago, E. M. Santos, W. J. C. Teves, and R. Zukanovich Funchal, Phys. Rev. D **63**, 073001 (2001); arXiv:hep-ph/0208166.

[27] M. Cirelli, G. Marandella, A. Strumia, and F. Vissani, Nucl. Phys. **B708**, 215 (2005); A. Y. Smirnov and R. Zukanovich Funchal, Phys. Rev. D **74**, 013001 (2006).

[28] M. Gasperini, Phys. Rev. D **38**, 2635 (1988); M.

Gasperini, Phys. Rev. D **39**, 3606 (1989); S. L. Glashow, A. Halprin, P. I. Krastev, C. N. Leung, and J. T. Pantaleone, Phys. Rev. D **56**, 2433 (1997); S. R. Coleman and S. L. Glashow, Phys. Rev. D **59**, 116008 (1999); H. Minakata and H. Nunokawa, Phys. Rev. D **51**, 6625 (1995); G. L. Fogli, E. Lisi, A. Marrone, and G. Scioscia, Phys. Rev. D **60**, 053006 (1999).

[29] L. Okun, Sov. J. Nucl. Phys. **10**, 206 (1969); Phys. Lett. B **382**, 389 (1996); J. A. Grifols and E. Masso, Phys. Lett. B **396**, 201 (1997); **579**, 123 (2004); M. C. Gonzalez-Garcia, P. C. de Holanda, E. Masso, and R. Zukanovich Funchal, J. Cosmol. Astropart. Phys. 01 (2007) 005.

[30] G. R. Dvali and A. Y. Smirnov, Nucl. Phys. **B563**, 63 (1999).

[31] R. S. Raghavan, Neutrino Oscillation Workshop (NOW2006), Conca Specchiulla, Otranto, Lecce, Italy, 2006, http://www.ba.infn.it/~now2006/.

[32] W. Potzel, Phys. Scr. **T127**, 85 (2006).